PROCEEDINGS, 48th Workshop on Geothermal Reservoir Engineering
Stanford University, Stanford, California, February 6-8, 2023
SGP-TR-224

Seismic Study at the Mori Geothermal Power Plant, Japan using DAS and DTS in a geothermal well

Junzo Kasahara[1,2], Yoko Hasada[1,3], Hitoshi Mikada[4], Haruyasu Kuzume[1], Hiroshi Ohnuma[1] and Yoshihiro Fujise[5]

ENAA, 1-11-9 Azabudai, Minato-ku, Tokyo 106-0041, Japan

Kasahara.junzo@shizouka.ac.jp

1: ENAA, 1-11-9 Azabudai, Minato-ku, Tokyo 106-0041, Japan

2: Shizuoka Univ., Center for Integrated Research and Education of Natural Hazard, 836 Ohya, Suruga-ku, Shizuoka 422-8529, Japan

3: Daiwa Exploration and Consulting Co. Ltd., 5-10-4 Toyo, Koto-ku, Tokyo 135-0016, Japan

4: Kyoto Univ., Department of Earth Resources Engineering, Katsura, Nishikyo-ku, Kyoto 615-8530, Japan

5: WELMA Co. Ltd., 2-3-3, Watanabe Street, Chuo-ku, Fukuoka 810-0004, Japan

Keywords: DAS, DTS, geothermal field, seismic reflection, geothermal reservoirs, VSP

ABSTRACT

As the third field study using an optical fiber seismic sensor array in the geothermal well, we conducted geophysical exploration at the Mori geothermal field in Hokkaido, Japan. We used an optical fiber system in the geothermal well to the depth of 2,100 m located in the Nigorikawa caldera basin. Active seismic sources were deployed in the caldera basin surrounding the F-01 well, whose temperature profile showed a maximum temperature of 206 °C at the bottom of the well. The DAS seismic records with 30-second sweeps between 10 and 75 Hz 500 times were stacked. The DAS records indicate numerous seismic reflected phases below 1,000 m depth, the first arrival discontinuity at 1,060 m, and the P first arrival amplitude attenuation below 1,060 m depth. We conducted the Vp travel-time tomography along the east-west and north-south lines using the P fist arrivals of DAS and surface seismometers data. The observed travel time discontinuity was partly explained by the model of a rectangular shape zone of 50 m thick and 250 m long filled with water at the 1,060 m depth. The layer at 1,060 m could be caused by the vertical fracture zones filled with the injected wastewater and pre-existing water-filled fractures before injection. We also made the migration image along the east-west line using DAS reflection arrivals. The seismic reflection zones at a depth between 2,000 and 3,000 m imply a fracture system located in the production zone of the power plant. The current results can well explain the existing geothermal data owed by the Mori Geothermal Power Plant.

1. INTRODUCTION

Geothermal energy is getting essential for renewable energy, particularly in Japan. However, we notice several problems in geothermal development. One of the most important things is to drill the best place to get geothermal energy to avoid the failures of drilling. In addition, world geothermal people (Dobson *et al.*, 2017; Reinsch *et al.*, 2017) and the Japanese governmental agency of NEDO (New Energy and Industrial Technology Development Organization) in Japan propose using supercritical water for new geothermal energy resources. The supercritical reservoir could be more profound than the 3 km depth because the critical point of the pure supercritical water is 374.1 °C and 22.06 MPa. For solving the above two significant problems, it is necessary to establish an accurate method for determining the geothermal reservoirs, which can be applied to the deeper reservoirs as 3km.

To determine the plausible location for the supercritical geothermal reservoirs, we have worked to develop the best technologies since 2017. We have used the DTS (Distributed Temperature Sensor) and DAS (Distributed Acoustic Sensor) (Hartog, 2017) in the geothermal wells to measure the temperature profile of the well and seismic structures in the geothermal field. We use both natural earthquakes and artificial seismic sources for seismic exploration. We explored geothermal characteristics using these technologies at Medipolis (Kasahara *et al.*, 2019a, b;2020a, b), Ohnuma (Kasahara *et al.*, 2022a), Mori, Sumikawa (Kasahara *et al.*, 2022b), Takigami (Kasahara *et al.*, 2022c), and Kijiyama geothermal fields between 2018 and 2022. This paper describes the case study of the Mori geothermal plant in Hokkaido, Japan, in 2021.

2. GEOLOGICAL AND GEOTHERMAL CHARACTERISTICS OF MORI GEOTHERM

In 2021, we conducted a geophysical study using DTS and DAS in the Mori geothermal Power Plant field. We used the single-mode optical fiber system in the F-01 geothermal well of the Mori Geothermal Power Plant. The F-01 geothermal well is located in Mori town on Hokkaido Island in Japan (Fig. 1). The Mori Geothermal Power Plant is owned by Hokkaido Electric Power Co., producing 25 MW

of electricity. The bottom depth of the F-01 well is 2,100 m. The Mori geothermal field's geothermal production and injection wells are located in the Nigorikawa caldera basin.

NEDO drilled three exploration wells in the Nigorikawa caldera basin. They obtained the geological description of the three wells shown in Fig. 3. The caldera is filled and volcanic rocks surrounded by Tertiary and pre-Tertiary chart and limestone layers (Kurozumi and Doi, 2003). The Nigorikawa caldera is nearly flat at 109-120 m in latitude. The caldera was thought to be a funnel shape (Ando *et al.*, 1992). Kurozumi and Doi (2003) and Hanano et al. (2005) presented the geological and geothermal models for Nigorikawa geothermal field. By their model, we can recognize the injection and production zones.

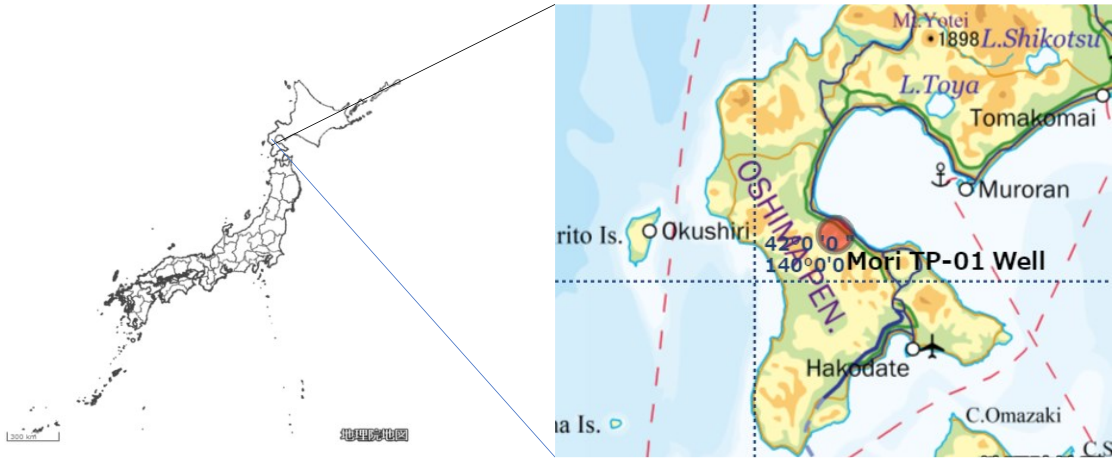

Figure 1: This diagram shows the location of the Mori-geothermal field in Hokkaido, Japan (solid red square). (Left) Map of Japan. (Right) the portion of Hokkaido, including the Mori (Nigorikawa) geothermal field. The map is based on the digital map published by the Geospatial Information Authority of Japan.

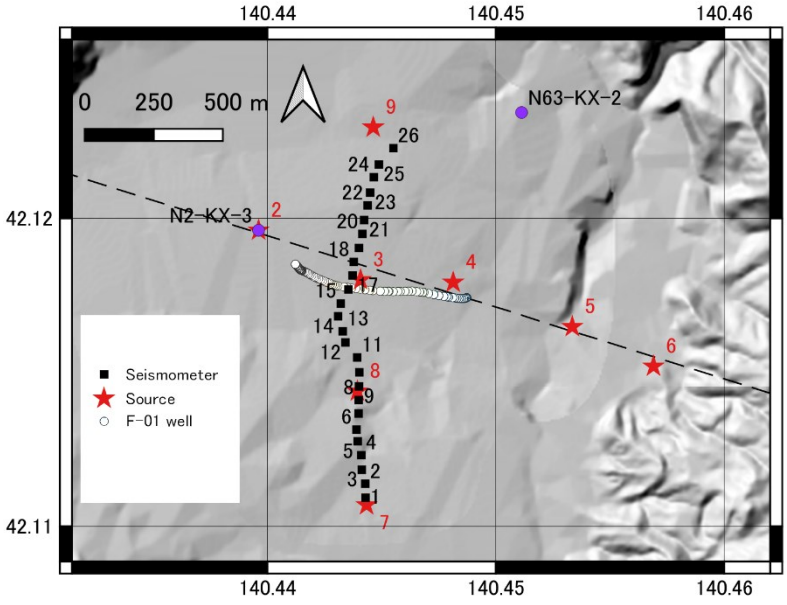

Figure 2: Location map of the trajectory of the F-01 well (circles), seismic sources (red stars), and surface seismometers (solid black squares). The purple star and solid circles are the NEDO-N2 KX-3 and N63-KX-2 exploration wells (NEDO, 1993). The F-01 geothermal well is located in the Nigorikawa caldera basin. The black broken line was used for the Vp tomography analysis.

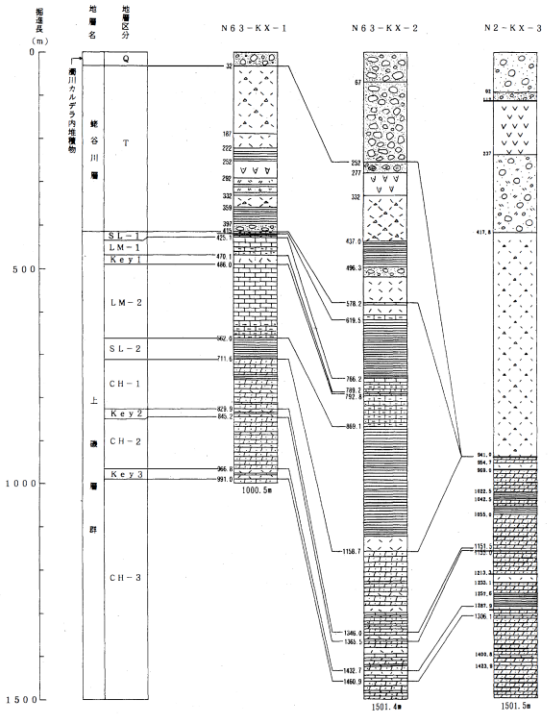

Figure 3: The geological sections of three wells obtained by the NEDO exploratory well (NEDO, 1993). The location of H63-KX-2 and N2-KX-3 is shown in Fig. 2. At the N2-KX-3, the layer shallower than 112 m is sediments. The layers to 237 m, 417.8 m, 941 m and deeper depth are andesitic lava, tuff breccia and clay, tuff breccia, and upper Kamiiso formation (chart, slate and breccia).

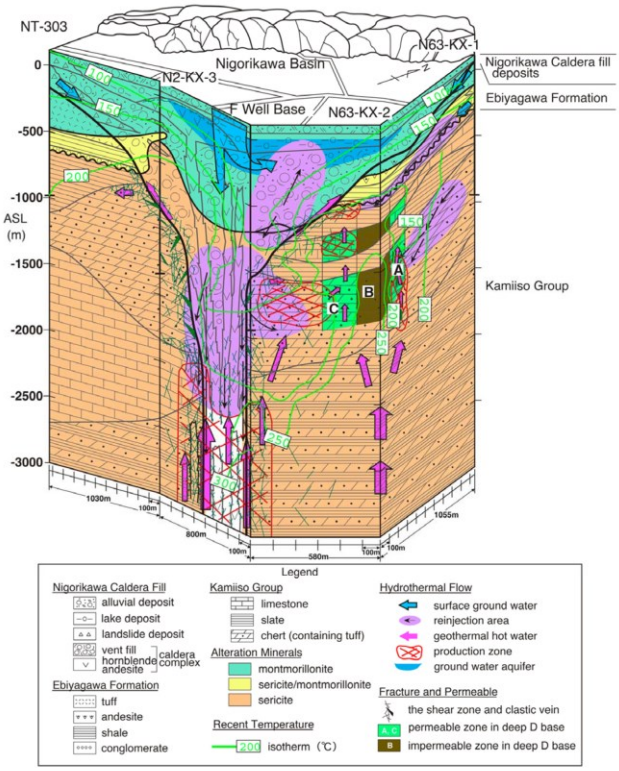

Figure 4: shows the Nigorikawa caldera model by Hanano *et al.* (2005). The production and injection zones are 2,000-3,000 m depth and 1,000 m depth, respectively.

3. FIELD OBSERVATION AND DATA PROCESSING

We show the profile of the F-01 geothermal well, locations of eight seismic sources, and surface seismometers in Fig. 2. We installed the single-mode optical fiber system to 2,100 m depth in the F-01 geothermal well. The polyimide coating optical fiber was in dual stainless tubes armed by tension members. Fig.3 also shows two NEDO experimental wells (N63-FX-2 and N2-FX-3) in the same diagram. The N2-KX-3 is close to the SP2 seismic source. The bottom of the F-01 well is outside of the caldera structure. We obtained the DAS seismic and DTS temperature records at 2,000 m and 2,100 m depth, respectively. We also obtained seismic data using surface seismometers in the Nigorikawa caldera basin (Fig. 2). We acquired continuous seismic records using DAS and surface seismometers from May 13 to June 1, 2022.

We placed eight seismic source points in the caldera basin for emitting sweep seismic signals for 500 times at each source location. The source signal was designed as a frequency upsweep from 10 to 75 Hz for 30 seconds, followed by an interval time of 30 seconds. We performed weighed stacking for 500 sweep records and deconvolved each stacked record with the source signature to get a flat spectrum response. The weight was chosen based on the noise level of every sweep record.

The P first arrivals readings of the stacked DAS and surface seismometer data were used for travel time topography analysis. We applied the f-k filtering to DAS records to separate them from direct arrivals and reflections for the migration process. The down-going and upgoing arrivals correspond to direct and reflected ones, respectively.

4. RESULTS

We obtained the well's temperature profile and DAS seismic records by DTS and DAS methods, respectively. The DAS and surface seismometers obtained eight seismic excitations and natural earthquakes.

4.1 Temperature profile

We obtained the temperature profile of the TP-2 well (Kasahara *et al.*, 2022d). The maximum temperate was 206˚C near the bottom of the well. The upper 60 m and the rest of the well were filled with air and water, respectively. The temperature profile shows the temperature gradient increase initiated around the 700 m depth. The temperature profile was very similar to the data previously measured by the Hokkaido Electric Company.

4.2 Seismic results

We obtained DAS records for eight seismic sources. Five original DAS records and their f-k filtering results along the E-W line are shown in Figs. 5-7. We can recognize the presence of numerous reflections and arrival gaps around 1,000 m depth. At the 1,060 m depth, P first arrivals are discontinuous to the deeper arrivals than the 1,060 m depth. The P first arrival amplitudes show attenuation below 1,060 m depth. We also have multiple reflections around this depth.

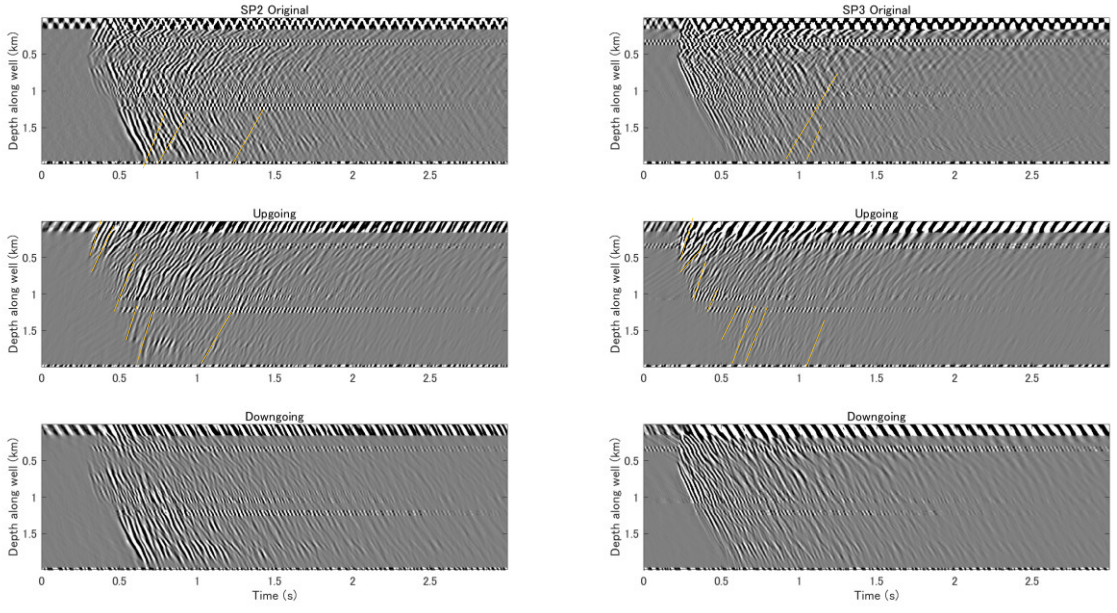

Figure 5: DAS records and their f-k filtering ones. (Left) the DAS records for the SP2. (Right) the DAS records for the SP3. Each diagram's horizontal and vertical axis is the elapsed times in seconds and the depth in the well in km, respectively. Three diagrams of each side are (top) original, (middle) upgoing, and (bottom) down-going phases. Yellow lines are reflected P arrivals.

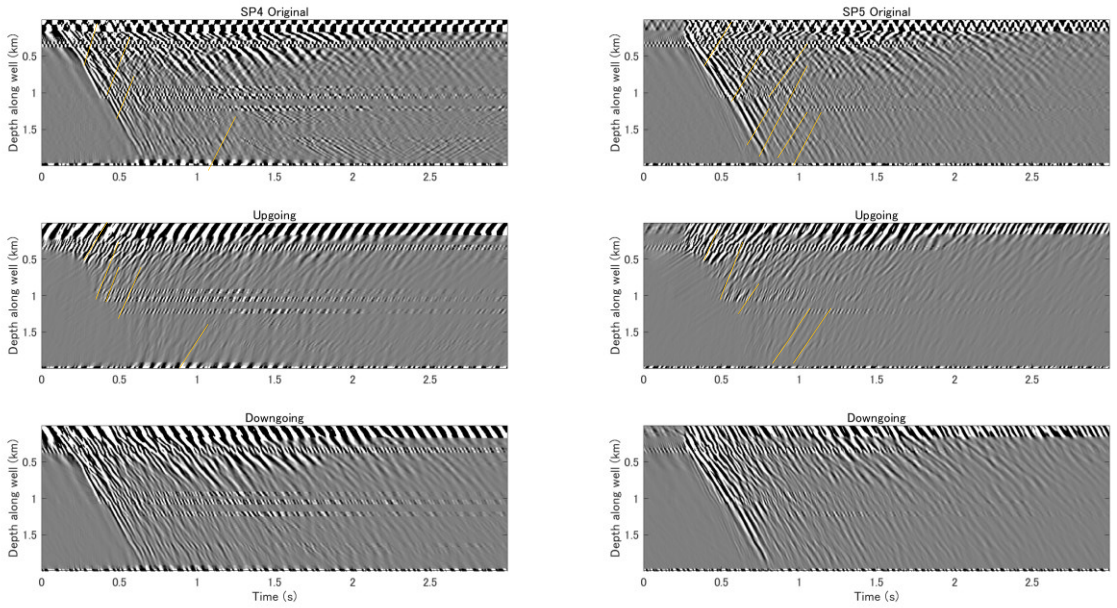

Figure 6: DAS records and their f-k filtering ones. (Left) The DAS records for the SP4. (Right) The DAS records for the SP5. Each diagram's horizontal and vertical axis is the elapsed times in seconds and the depth in the well in km, respectively. Three diagrams of each side are (top) original, (middle) upgoing, and (bottom) down-going phases. Yellow lines are reflected P arrivals.

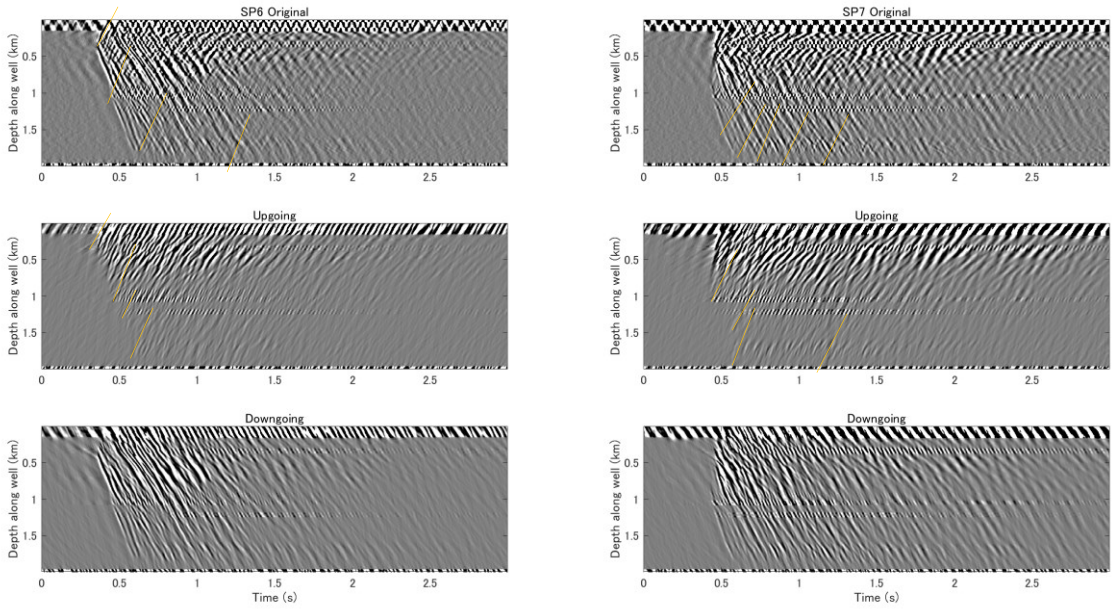

Figure 7: DAS records and their f-k filtering ones. The DAS records for SP6. Each diagram's horizontal and vertical axis is the elapsed times in seconds and the depth in the well in km, respectively. Three diagrams of each side are (top) original, (middle) upgoing, and (bottom) down-going phases. Yellow lines are reflected P arrivals.

The P first arrival times of the DAS records and surface seismometers for eight seismic sources were used to get the Vp structure in the Nigorikawa caldera basin (Fig. 8). The high Vp portion at the shallow part appeared between SP2 and SP3, and is considered as the igneous body intruded to the shallow part.

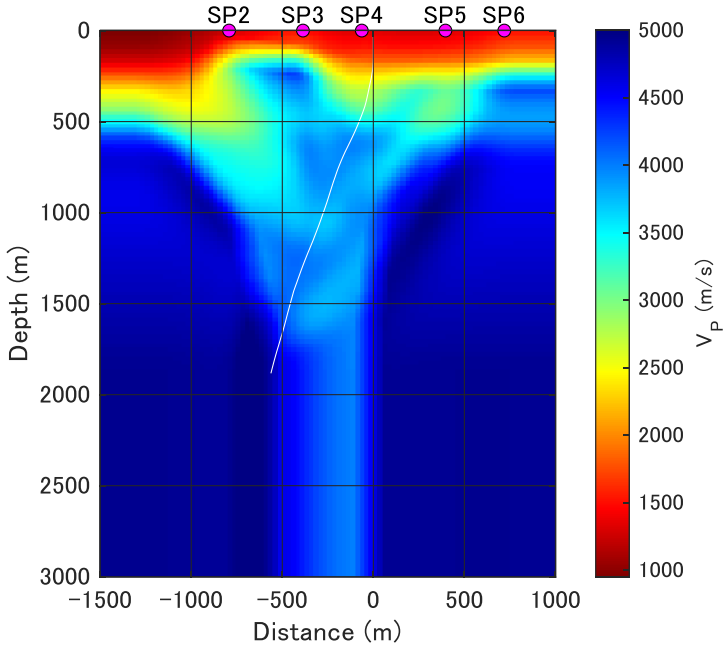

Figure 8: (Right) the Vp depth section along the EW line shown in Fig. 2 obtained by the DAS and surface seismometer first P arrivals. The white line shows the trajectory of the F-01 well. We call this the md00 model. (Left) temperature profile along the F-01 well.

5. INTERPRETATION OF DAS WAVEFORMS

The Vp structure and synthetic DAS waveforms for SP2-SP6 are demonstrated in Fig. 9 to Fig. 14. The md001 is the original Vp structure. The model md00 does not show the seismic characteristic at depths of 1,060 m and deeper. The m00 synthetics do not offer the travel time gap at 1,060 m and attenuation of amplitudes below 1,060 m depth. The reason can be that the P first arrivals do not satisfy amplitude information in the seismic tomography well.

We placed square(s) or rectangular with different physical properties in the surrounding zone at 1,060 m depth. We examined several models to satisfy the characteristic of a 1,060 m depth. The three of several models are shown in Fig. 9 and Table 1. The synthetic DAS waveforms for these models are shown in Figs. 10-14 and Table 1. The md00 shows the Vp structure, and the Vs distribution is derived using travel time tomography. In model md01, we placed three vertical zones filled with low Vp and Vs materials. The model md03 has a rectangular water layer of 250 m long in width and 50m in thickness at 1,060 m depth. The model md04 has three square-shaped anomalies filled with water of a 50 m side length at 1,060 m depth.

Table 1: This shows five structure models. The md00 is the original Vp model with assuming Vs and density.

Model name	Width (m)	Height (m)	Velocity(km/s)		
			Vp	Vs	Layer(s) at 1060 m depth
md00					
md01	50	300	3.5	2	Three layers with 50 m spacing
md03	250	50	1.5	0	One layer
md04	50	50	1.5	0	Three layers with 50 m spacing

The synthetic waveforms using md00 do not show the distinct P first arrival gap at 1,060 m depth and attenuated amplitudes below 1,060 m depth. Among the other three models, the md03 is the best-fitting characteristic of the observed DAS records, especially at 1,060 m depth.

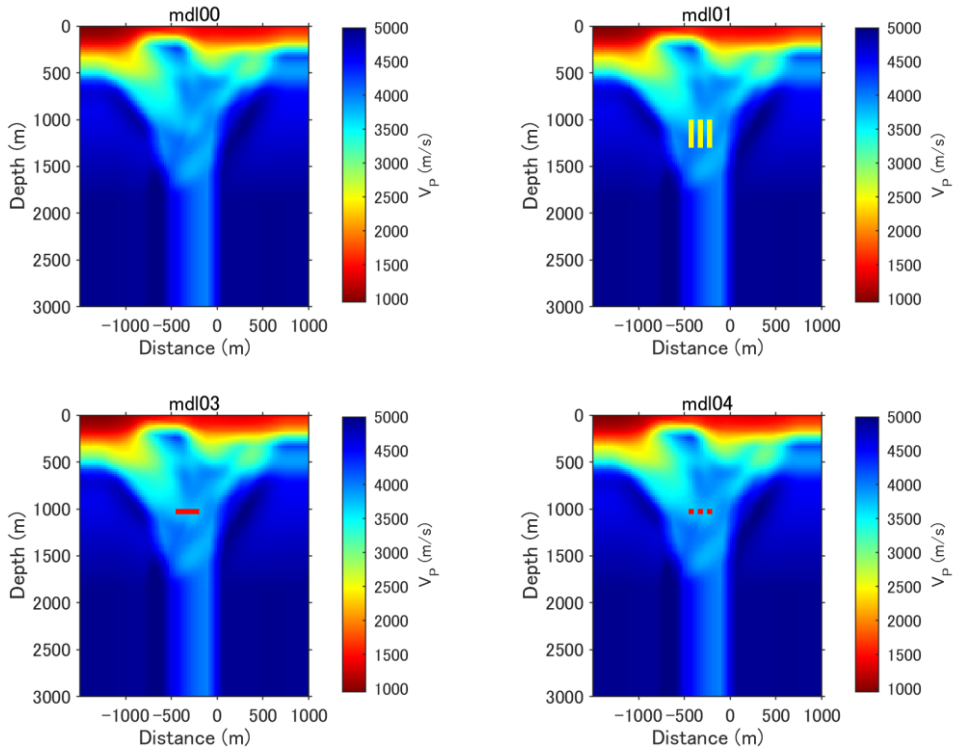

Figure 9: Models (md00, md01, md03, and md04) synthetic DAS waveform calculation.

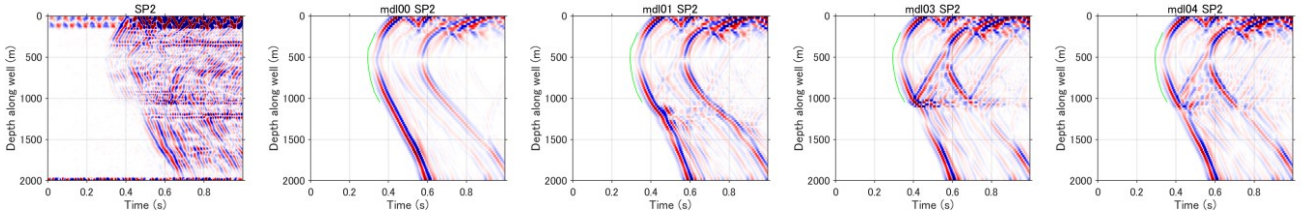

Figure 10: Synthetic DAS waveforms of five seismic source locations (SP2) for the original and four models are shown in Fig. 10.

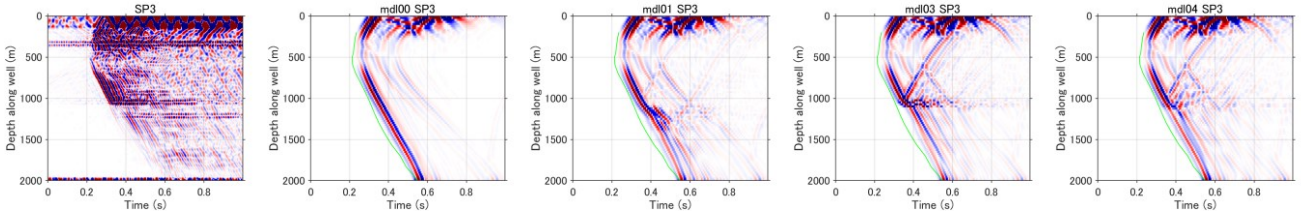

Figure. 11: Synthetic DAS waveforms of five seismic source locations (SP3) for the original and four models are shown in Fig. 10.

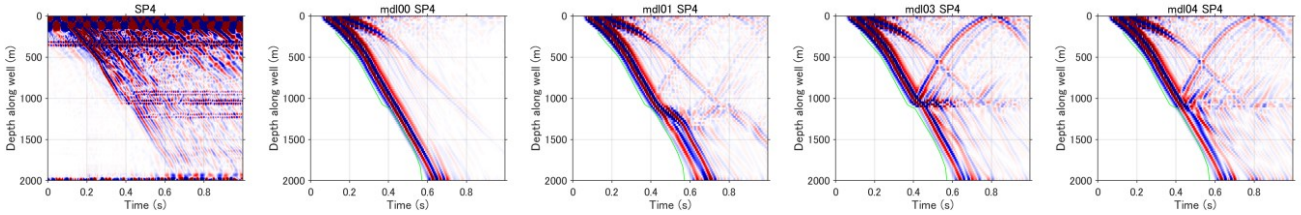

Figure. 12: Synthetic DAS waveforms of five seismic source locations (SP4) for the original and four models are shown in Fig. 10.

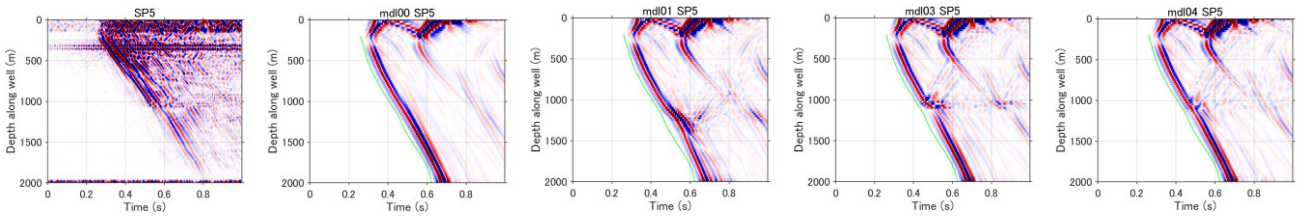

Figure. 13: Synthetic DAS waveforms of five seismic source locations (SP5) for the original and four models are shown in Fig. 10.

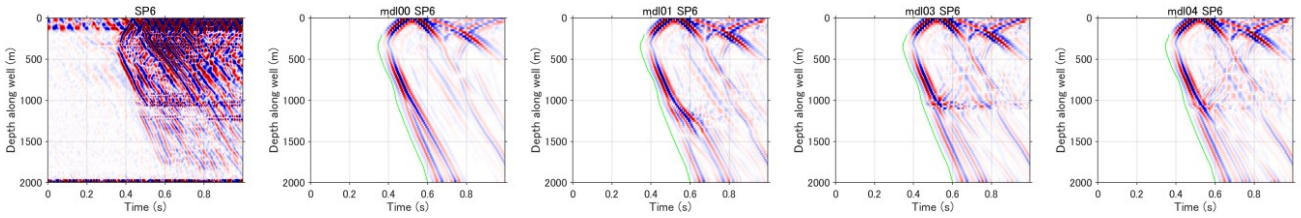

Figure. 14: Synthetic DAS waveforms of five seismic source locations (SP6) for the original and four models are shown in Fig. 10.

6. IMAGING OF REFLECTED PHASES

In the next step, we made a migration image using the DAS records (SP2-SP6) along the E-W line shown in Fig. 2. The results are shown in Fig. 15. We can see reflection zones from 1,500 m to 3,000 m depth.

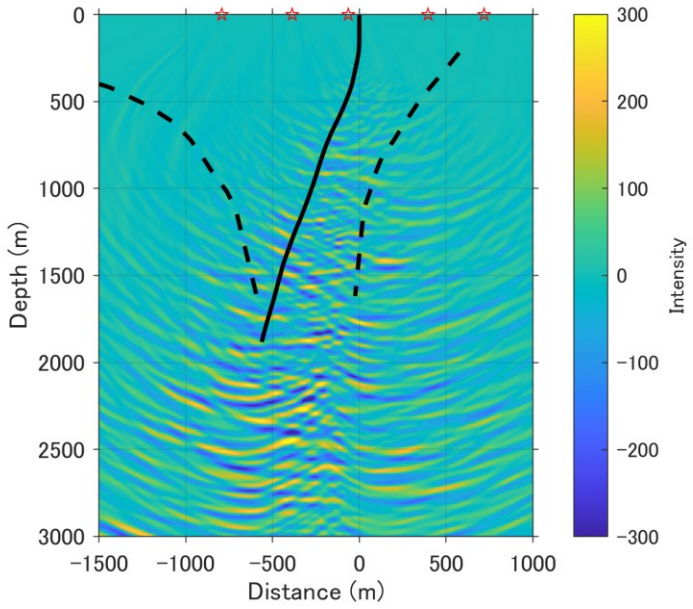

Figure 15: Results of image migration for the reflection arrivals along the E-W line and the N-S road are shown in Fig. 2. The broken lines are estimated caldera wall, and the solid black line is the trajectory of the F-01 well.

7. DISCUSSION AND CONCLUSIONS

We obtained the Vp profile of the Nigorikawa caldera basin along the E-W line using DAS records in the F-01 well to 2,000 m and surface seismometer records. The observed DAS records show a distinct P first arrival gap and amplitude attenuation below 1,060 m depth. The waveform characteristics of DAS observation at 1,060 m and below were examined by structural models with low Vp and VS zones around 1,060 m. The better model among the three models is md03, which has a rectangular box filled with water at 1,060 m depth. Although this rectangular zone is a bit artificial, this might fit the injection of wastewater at this depth. This observation might explain the reason for the model at 1,060 m depth. The Vp structure of md03 obtained in this study in Fig. 10 is well-fitted to past knowledge, such as density, injection zone, production zone, and permeability of the Mori geothermal area owned by the Hokkaido Electric Company (Kajiwara *et al.*,2022).

We can see numerous reflections between 1,000 m and 3,000 m depth in the migration image. The reflections between 1,000 m and 3,000 m show the fractures filling with hot water at this depth. The zone between 2,000 m and 3,000 m corresponds to the production zone. The location below 1,000 m corresponds to the injection zone. In addition, the DAS records show that travel time gap and attenuation below 1,060 m depth can be the top of reflection zones.

8. ACKNOWLEDGMENTS

We deeply thank the New Energy and Industrial Technology Development Organization (NEDO), who supported this study. This survey was done by the NEDO supercritical Development Project (JPNS21991). We greatly appreciate Hokkaido Electric Power Corporation's permission to conduct fieldwork at their power plant. We also thank WELMA Co., Ltd., Hanshin Consultants Co., and KGE Co. for their data acquisition assistance.

REFERENCES

Dobson, P., Asanuma, H., Huenges, E. Poletto, F., Reisch, T., and Sanjuan, B.: Supercritical geothermal system-A review of past studies and ongoing research activities, Proceeding 41st Workshop on Geothermal Reservoir Eng., Stanford Univ., Stanford, California, Feb. 13-15, 2017.

Hanano, M., Kajiwara, T., Hishi, Y., Arai, F., Asanuma, M., Sato, K. and Takanohashi, M.: Overview of Production at the Mori Geothermal Field, Japan, Proceedings World Geothermal Congress 2005, Antalya, Turkey, 24-29 April 2005.

Hartog, A. H.: An introduction to distributed optical fiber sensors, RC Press. 440 pp, 2017.

Kajiwara, T., Kasahara, J., Moriya, Y., Nagaso, N., Maetou, K. and Ohuma, H.: Comparison of DAS survey results with geological and geophysical model in the Mori Geothermal field, 2022 Annual Meeting Geothermal Research Society of Japan Abstract with program, A34, 2022.

Kasahara, J., Hasada, Y. and Yamaguchi, T.: Seismic imaging of supercritical geothermal reservoir using full-waveform inversion method, Proc. 44th Workshop on Geothermal Reservoir Engineering, Stanford University, Stanford, CA, 2019a.

Kasahara, J., Hasada, Y., Kuzume, H., Fujise, Y. and Yamaguchi, Y.: Seismic feasibility study to identify supercritical geothermal reservoirs in a geothermal borehole using DTS and DAS, EAGE extended abstract, EAGE 2019 Annual Meeting, London, 2019b.

Kasahara, J., Hasada, Y., Kuzume, H., Mikada, H. and Fujise, Y.: The second seismic study at the geothermal field in southern Kyushu, Japan using an optical fiber system and surface geophones, Proc. 44th Workshop on Geothermal Reservoir Engineering, Stanford University, Stanford, CA, 2020a.

Kasahara, J.,Hasada, Y., and Kuzume, H. : Possibility of high Vp/Vs zone in the geothermal field suggested by the P-to-S conversion, Proc. 44th Workshop on Geothermal Reservoir Engineering, Stanford University, Stanford, CA, 2020b.

Kasahara, J., Hasada, Y., Kuzume, H. Mikada, H. and Fujise, Y.: The DAS geothermal study in the geothermal borehole of the Ohnuma geothermal power plant in Hachimantai, Honshu, Japan, Jour. The Geothermal Research Society of Japan, 44(2), 2022a.

Kasahara, J., Hasada, Y., Ohnuma, H., Mikada H. and Fujise, Y.: Geothermal exploration in the Sumikawa geothermal field using optical fiber system in the geothermal well, 2022 Annual Meeting Geothermal Research Society of Japan Abstract with program, P45., 2022b.

Kasahara, J., Hasada, Y., Furuya, S., Shimazaki, M., Ohnuma, H., Mikada, H. and Fujise, Y.: Geothermal exploration in the Takigami geothermal field using the optical five system in the geothermal well, 2022 Annual Meeting Geothermal Research Society of Japan Abstract with program, A41., 2022c.

Kasahara, J., Hasdada, Y., Kuzuma, H., Ohnuma, H. Mikada, H. and Fujise, Y.: A field experiment of a temperature-tolerant distributed acouste sensor in deep geothermal reservoir prospecting, The Leading Edge, May 2022, 306-31, 2022d.

Kurozumi, H. and Doi, N.: Inner Structure of the Nigorikawa Caldera, Hokkaido, Japan, Bull. Volcanology Society Japan, III, 48, 259–274 (in Japanese), 2003.

New Energy Industrial Technology Development Organization (NEDO): Geothermal Development Promotion Survey Report of Mori Area, Summary volume, 444 p., 1993. (in Japanese).

Reinsch, T., Dobson, P., Asanuma, H., Huenges, E., Poletto, F. and B. Sanjuan, B.: Utilizing supercritical geothermal systems: a review of past ventures and ongoing research activities, Geothermal Energy, https://doi.org/10.1186/s40517-017-0075-y, 5, Article number: 16, 2017.